AIP Applied Physics Letters

Resonance frequency-retuned quartz tuning fork as a force sensor for noncontact atomic force microscopy

Hiroaki Ooe, Tatsuya Sakuishi, Makoto Nogami, Masahiko Tomitori, and Toyoko Arai

Citation: Applied Physics Letters **105**, 043107 (2014); doi: 10.1063/1.4891882
View online: http://dx.doi.org/10.1063/1.4891882
View Table of Contents: http://scitation.aip.org/content/aip/journal/apl/105/4?ver=pdfcov
Published by the AIP Publishing

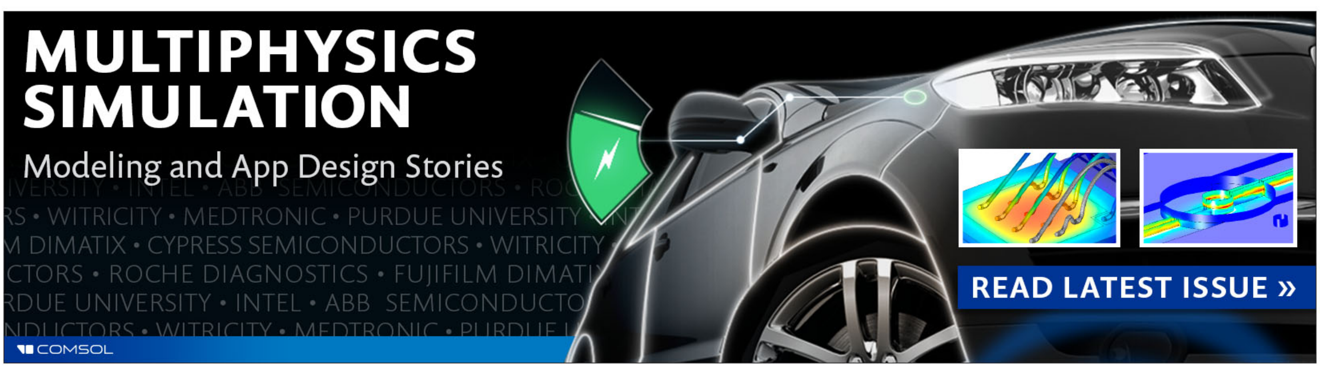

APPLIED PHYSICS LETTERS **105**, 043107 (2014)

Resonance frequency-retuned quartz tuning fork as a force sensor for noncontact atomic force microscopy

Hiroaki Ooe,[1] Tatsuya Sakuishi,[1] Makoto Nogami,[2] Masahiko Tomitori,[2] and Toyoko Arai[1,a)]
[1]*Natural Science and Technology, Kanazawa University, Kanazawa, Ishikawa 920-1192, Japan*
[2]*Japan Advanced Institute of Science and Technology, Nomi, Ishikawa 923-1292, Japan*

(Received 16 June 2014; accepted 21 July 2014; published online 30 July 2014)

Based on a two-prong type quartz tuning fork, a force sensor with a high Q factor, which we call a retuned fork sensor, was developed for non-contact atomic force microscopy (nc-AFM) with atomic resolution. By cutting a small notch and attaching an AFM tip to one prong, its resonance frequency can be retuned to that of the other intact prong. In balancing the two prongs in this manner, a high Q factor (>50 000 in ultrahigh vacuum) is obtained for the sensor. An atomic resolution image of the Si(111)-7 × 7 surface was demonstrated using an nc-AFM with the sensor. The dependence of the Q factor on resonance frequency of the sensor and the long-range force between tip and sample were measured and analyzed in view of the various dissipation channels. Dissipation in the signal detection circuit turned out to be mainly limited by the total Q factor of the nc-AFM system.
[http://dx.doi.org/10.1063/1.4891882]

Non-contact atomic force microscopy (nc-AFM)[1] is a powerful technique to observe sample surfaces on an atomic scale through the detection of the forces between sample and tip on an oscillating cantilever.[2,3] To describe the atom-scale short-range forces between them, the oscillation amplitude should be as small as possible at close separations between tip and sample because the forces range only over nanometer separations.[4] To operate stably, a high spring constant is required for the cantilever (force sensor) to avoid jump-to-contact behavior.[5]

Cantilevers with high spring constants have been fabricated using single-crystal quartz with a high Young modulus. These are easily purchased commercially as high-quality oscillators. The high-force sensitivity and long-term stability of the nc-AFM imaging have been obtained using the force sensor of a quartz oscillator with a high Q factor and a low thermal drift in its resonance frequency. The Q factor dominates the minimum detection limit of the force differentiation $\delta F'_{\mathrm{min}}$ given by[1]

$$\delta F'_{\mathrm{min}} = \sqrt{4kk_BTB/\pi f_0 QA^2}, \quad (1)$$

where k is the spring constant of the force sensor, k_{B} is the Boltzmann constant, T is the temperature in Kelvin, B is the bandwidth of the detection system, f_0 is the resonance frequency of the force sensor, and A is the oscillation amplitude. $\delta F'_{\mathrm{min}}$ is proportional to $\sqrt{k/Q}$ at constant T, B, f_0, and A. Consequently, a high Q factor for the oscillator is necessary for high force sensitivity. A high Q factor means that the energy dissipation from mechanical oscillations of the oscillator is less. This is defined as $Q = 2\pi$ (oscillation energy stored in the oscillator)/(dissipation energy per oscillation cycle).

Up to now, two types of force sensors, based on quartz tuning forks as the oscillator with high Q factor, have been frequently used in nc-AFM. The tuning fork comprises two prongs joined at their ends; the resonance frequencies (f_{TF}) of the two prongs are precisely tuned to the same frequency (typically, $f_{\mathrm{TF}} = 32\,768$ Hz). One of the force sensors is a two-prong type,[6] and the other is a single-prong type, called the qPlus sensor.[7] The Q factor of the tuning fork in its resonant state, the anti-phase oscillation mode of the two prongs, is greater than that in the in-phase oscillation mode and that for the one-prong sensor. This is because the anti-phase mode cancels the distortional oscillation amplitude at the join, leading to low energy dissipation at the join. However, when an AFM tip is attached to one prong, the oscillations of two prongs become unbalanced through the detuning of the resonance frequencies of the prongs, resulting in a lower Q factor.[6] To overcome this problem, Giessibl developed the qPlus sensor by fixing one prong, so that it would not oscillate, and observed atom-resolved images of Si(111)–7 × 7 using the oscillation of the other prong.[8] In contrast, the two-prong force sensors with a tip imaged only step structures of Si(111)[6] and highly ordered pyrolytic graphite.[9] To date, the high Q factor of a tuning fork has not been well exploited in nc-AFM.

For this study, we fabricated a two-prong force sensor with a high Q factor, which we call a retuned fork sensor, by retuning the resonance frequency of the prong with the AFM tip to that of the other intact prong. The imbalance caused by attaching the tip is cancelled by cutting a notch into the prong. A resonance state with a high Q factor is thereby restored. Atomic resolution images of Si(111)–7 × 7 were obtained with the sensor.

A quartz tuning fork oscillator (MS1V, Micro Crystal AG, Grenchen, Switzerland) in a metal can was used for the retuned fork sensor. The spring constant of the one prong was calculated from its size to be 1800 N/m.[8] f_{TF} and Q in the can measured 32 768 Hz and ~60 000, respectively. Fabrication of the sensor is depicted in Fig. 1. After

a)Electronic mail: arai@staff.kanazawa-u.ac.jp

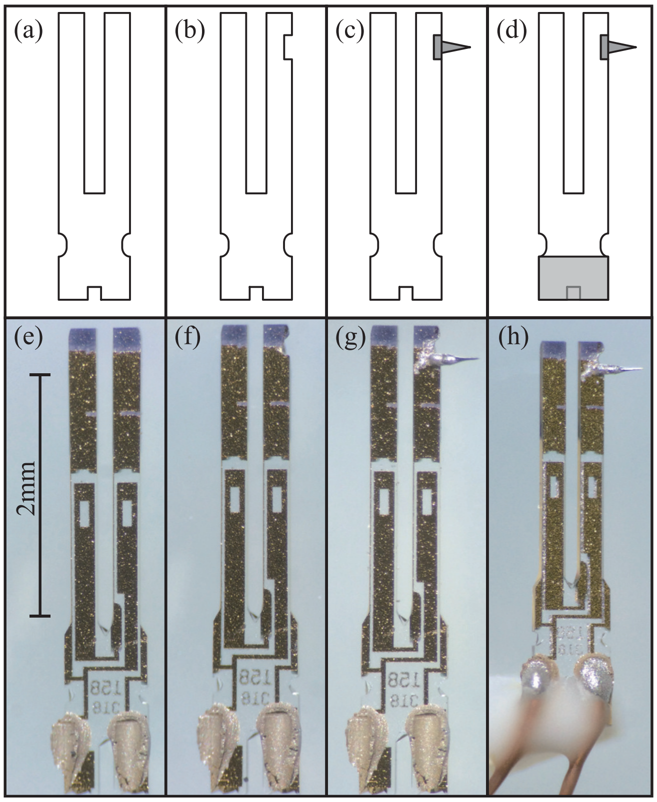

FIG. 1. Schematic of retuned fork sensor fabrication. (a) A typical quartz tuning fork. (b) A notch is cut at the end of one prong. (c) A tip is attached in the notch. (d) The hatched lower part of the tuning fork is fixed to a base. (e)–(h) Optical microscope photos corresponding to (a)–(d).

extracting the tuning fork from the can by breaking the bottom with pliers (Figs. 1(a) and 1(e)), a notch in the free end of one prong was filed down using a sewing needle (Figs. 1(b) and 1(f)), where a tip was attached with silver paste (Figs. 1(c) and 1(g)). Depending on tip and notch sizes, the amount of silver paste used provided the fine retuning. The tip was made by electrochemically etching of a W wire with a diameter of 100 μm for a tip radius of a few μm. In Fig. 1(d), the hatched region below the neck was used to fix the fork to a base and electric wires to electrodes so as not to lower the Q factor.

The resonance frequencies of the retuned fork sensor free from and under force are denoted by f_{RT0} and f_{RT}, respectively. In retuning, f_{RT0} can be adjusted to a lower or higher frequency than the resonance frequency of the intact prong, i.e., f_{TF}. When a negative resonance frequency shift Δf ($=f_{RT} - f_{RT0}$) for the nc-AFM imaging is needed, roughly in the attractive force regime, f_{RT0} will be set higher than f_{TF} by a specified quantity Δf for a target value for the nc-AFM feedback; when a positive shift Δf is needed in the repulsive force regime, f_{RT0} will be set lower than f_{TF} by a corresponding specified quantity Δf. Consequently, nc-AFM imaging can be conducted under a force at $f_{RT} \cong f_{TF}$, for which a high Q factor can be obtained for imaging.

To use the high Q factor of the tuning fork, the two prongs should be excited in the anti-phase mode. However, a dither piezoelectric plate, frequently used for mechanical excitation, more easily excites the in-phase oscillation of the two prongs. Meanwhile, commercial tuning forks are designed to excite the anti-phase mode by configuring the two sets of electrodes on the two prongs. In this study, we used one set for excitation by applying a sinusoidal signal and the other set for detection of the displacement signal of the tuning fork by connecting it to an operational amplifier. Because of stray capacitance across the two sets of electrodes, the sinusoidal signal leaks at the output of the amplifier. Thus, an electric circuit with a pulse transformer was used to measure the oscillation signal to reduce the leakage signal as well as to excite the anti-phase mode.[10] This circuit generates the anti-phase sinusoidal signals with the same amplitude, one of which excites the oscillation of the tuning fork; the other is used to cancel the leaked signal by adding the signal to the input of the amplifier through a capacitor adjustable to the stray capacitor. An operational amplifier (AD744, Analog Devices, Norwood, MA, USA) with a gain of 30×10^6 V/A was installed as the preamplifier, located near the force sensor in an ultrahigh vacuum (UHV) chamber for the nc-AFM. The sensitivity of the prong displacement of 0.6 nA/nm with a floor noise density of about 80 fm/$\sqrt{\text{Hz}}$ was evaluated by thermal vibration spectrum analysis. We employed a home-made nc-AFM combined with a scanning tunneling microscope operated in 1.5×10^{-10} Torr using the retuned fork sensor with the W tip. The sample was a Si(111)–7×7 surface cleaned by flashing in the UHV.

Figure 2(a) shows an atom-resolved Δf image of Si(111)–7×7 obtained using our retuned fork sensor in the constant-height nc-AFM mode. A simultaneously obtained time-averaged tunneling current ($\langle I \rangle$)[11] image also exhibited atomic resolution (Fig. 2(b)); f_{RT0} was 32 877 Hz with a Q factor of about 18 000. Note that the measured Q factor seemed to be limited by the detection circuit (details are discussed later). The contrast in the Δf image indicates that the attractive force over Si adatoms was weaker with larger current. This change in Δf is attributed to the decrease in electric potential over the Si adatoms, where an Ohmic voltage drop appeared in the circuit because the current increased over the Si adatoms. This was interpreted as a weakening of the electrostatic force between the tip and the Si adatoms as the electric potential decreased; this is the so-called phantom force.[12]

We measured the resonance properties of 24 retuned fork sensors each with a tip and with different f_{RT0}. Figure 3 shows the plots of their Q factors versus $f_{RT0} - f_{TF}$ in air (a) and in UHV (b). The Q factor, measured by sweeping the frequency of excitation signal, increased as $f_{RT0} - f_{TF}$

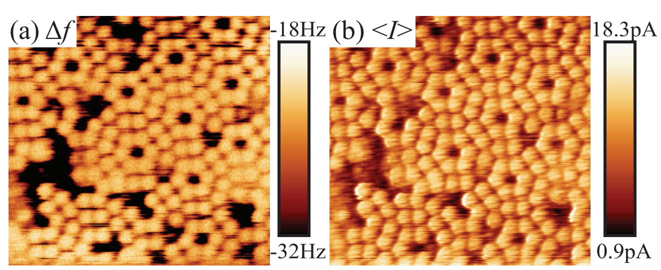

FIG. 2. (a) Resonance frequency shift (Δf) image of Si(111)-7×7 in a constant height mode observed with a retuned fork sensor. The averaged Δf was about -25 Hz. Brighter means positive increase in Δf. Scan area was 10 nm $\times$ 10 nm. (b) Simultaneously obtained average current image $\langle I \rangle$. Imaging conditions: $V_{sample} = 2$ V, oscillation amplitude $A = 1$ nm.

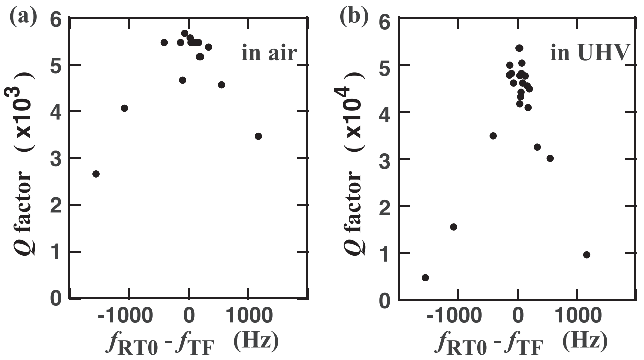

FIG. 3. Plots of Q factor versus $f_{RT0} - f_{TF}$ measured (a) in air and (b) in UHV with retuned fork sensors with different f_{RT0}; on one prong a tiny mass was added or a notch was cut. Note: f_{TF} is the resonance frequency of the other intact prong, i.e., that for the original tuning fork (=32,768 Hz).

approached zero. The plots are mirror-symmetric about the zero; the frequency change $|f_{RT0} - f_{TF}|$, caused by adding/subtracting to the prong, decreased the Q factor irrespective of sign ($f_{RT0} - f_{TF} > 0$ for extracting, and <0 for appending); Rychen described similar results adding mass to one prong.[13] With both signs for $f_{RT0} - f_{TF}$ (Fig. 3), the Q factor is clearly maximized by retuning f_{RT0} to f_{TF}, i.e., the resonance frequency of an intact prong. The Q factor was about 5500 in air and 50 000 in UHV at maximum, and barely changed in the range ±400 Hz in air and ±200 Hz in UHV. Note that we were able to retune a force sensor with a high Q factor for a tip as large as a few hundred μm in length and 100 μm in diameter. Previous methods only attached tips that were as small as possible to limit the imbalance between the two prongs.[13]

According to the mechanics of oscillation, the inverse of the Q factor represents the quantity proportional to the dissipation of oscillation energy per cycle, decomposed into several terms depending on origin

$$1/Q_{eff} = 1/Q_{mech} + 1/Q_{ele} + 1/Q_{air} + 1/Q_{Joule} + 1/Q_{ts}. \quad (2)$$

Here, $1/Q_{eff}$ is the measured $1/Q$ value, $1/Q_{mech}$ corresponds to the energy dissipation of the mechanical oscillation in the oscillator, $1/Q_{ele}$ to the energy dissipation in the electric circuit that excites and detects the oscillation, $1/Q_{air}$ to the energy dissipation from the viscosity of air surrounding the oscillator, and $1/Q_{Joule}$ to the Joule heating across the resistor in the circuit caused by the displacement current passing between the tip and sample in oscillation under a bias voltage. $1/Q_{ts}$ corresponds to the energy dissipation through the tip-sample interaction, which can be ignored at a wide tip-sample separation on sub-μm scales. With no bias voltage and a wide separation between tip and sample, as depicted in Fig. 3, $1/Q_{Joule}$ and $1/Q_{ts}$ can be regarded zero.

We evaluated the respective terms of the Q factor and compared the plots in air (Fig. 3(a)) with those in UHV (Fig. 3(b)). Because each term except Q_{air} was of the same order in the measurements, the difference in Q_{eff} between them was ascribed to Q_{air}. According to Eq. (2), Q_{air} was estimated about 6000 in the range $f_{TF} \pm 400$ Hz. $1/Q_{mech}$ includes the energy transmission through the join between the two prongs. As the join does not oscillate in the anti-phase, the transmission is negligible around $f_{RT0} \sim f_{TF}$ so that Q_{mech} can be as high as a few hundred thousand, limited by the internal friction[14] of the quartz oscillator. However, the energy transmission cannot be ignored with unbalanced prongs due to the AFM tip or notch, which resulted in a lowered Q_{mech} with f_{RT0} deviating from f_{TF} (Fig. 3). Nevertheless, in the UHV, Q_{eff} seemed to be limited by Q_{ele}, roughly estimated to be 60 000; the value should be the same for the measurements in air. The oscillation energy possibly dissipates in the circuit because of the alternating current around the circuit, including the pulse transformer.

Next, the electric excitation signal required to maintain a constant oscillation amplitude for the force sensor was measured, and yields $1/Q_{eff}$ as a function of Δf for various tip-sample separations in UHV for the retuned fork sensor and the qPlus sensor (Fig. 4). We applied a high voltage of +5 V to the sample at a small amplitude ($A = 1$ nm) at a wide tip-sample separation, where only a long-range electrostatic force was dominant and less sensitive to the tip shape. At almost free oscillation, $f_{RT0} = 32\,784$ Hz ($f_{RT0} - f_{TF} = 16$ Hz) and $Q_{eff} = 54\,000$ for the retuned fork sensor, whereas the resonance frequency of the qPlus sensor (f_{qPlus0}) was 32 564 Hz with $Q_{eff} = 11\,000$. The excitation signal for both sensors increased almost linearly as Δf negatively increased, although $1/Q_{eff}$ for the retuned fork sensor had been expected to be minimum at $f_{RT} = f_{TF}$ ($\Delta f = -16$ Hz in Fig. 4), when the two prongs were balanced. This unexpected behavior was ascribed to the effect of $1/Q_{Joule}$ and $1/Q_{ele}$ evaluated below: here, r is the tip radius, z is the tip-sample distance ($z = z_0 + A\cos(2\pi ft)$, where z_0 is z at the center of the oscillation, and f is the oscillation frequency), and V is the sample bias voltage. When $z \ll r$ (in our measurements r is of μm order), the electrostatic force F_{el} can be approximated as[15]

$$F_{el} = -\pi\varepsilon_0 V^2 \frac{r}{z}, \quad (3)$$

where ε_0 is the dielectric constant in vacuum. We assumed that the amplitude A is much less than z, as the tip position is far from the dominant region of the short-range force. The resistance component of the detection circuit is denoted by R_J. The averaged Joule heat $\langle IV \rangle$ due to the displacement current I through an electric capacitor C between the tip and the sample over one oscillation cycle can be derived using

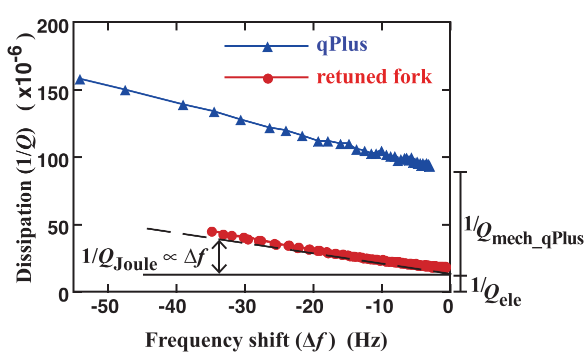

FIG. 4. Dissipation ($1/Q$) as a function of Δf in UHV for a qPlus sensor (blue curve) with $\Delta f = f_{qPlus} - f_{qPlus0}$, and for our retuned fork sensor (red curve) with $\Delta f = f_{RT} - f_{RT0}$. The spring constant k and resonance frequency of the qPlus sensor and the retuned fork sensor were 1800 N/m and $f_{qPlus0} = 32{,}564$ Hz, and 3600 N/m and $f_{RT0} = 32\,784$ Hz, respectively. The acquisition conditions: $V_{sample} = +5$ V and $A = 1$ nm.

$I = (dC/dt)V = (\partial C/\partial z)(dz/dt)V$ and $F_{el} = 1/2(\partial C/\partial z)V^2$. According to the above definition of the Q factor, $1/Q_{Joule} = \langle IV \rangle / \pi k A^2$; we obtain, finally

$$1/Q_{joule} = \frac{16\pi^3 \varepsilon_0^2 r^2 R_J f V^2}{kA^2} \frac{z_0 - \sqrt{z_0^2 - A^2}}{\sqrt{z_0^2 - A^2}}. \tag{4}$$

Using the Hamilton—Jacobi method,[16] we can derive the frequency shift Δf_{el} associated with F_{el} as follows:

$$\Delta f_{el} = \frac{\pi \varepsilon_0 r f_0 V^2}{kA^2} \frac{z_0^2 - A^2 - z_0\sqrt{z_0^2 - A^2}}{z_0^2 - A^2}. \tag{5}$$

Consequently, $1/Q_{Joule}$ is proportional to Δf_{el}: $1/Q_{Joule} \approx -16\pi^2 \varepsilon_0 r R_J \Delta f_{el}$, if Δf_{el} is sufficiently smaller than f_0. Accordingly, the linear change in $1/Q_{eff}$ with respect to Δf (Fig. 4) can be attributed to Q_{Joule} for both sensors. Note that the change in $1/Q_{eff}$ for the retuned fork sensor is slightly saturated as Δf approaches zero because $1/Q_{mech}$ of the retuned fork sensor became noticeable as the two prongs were unbalanced far from $f_{RT} = f_{TF}$ ($\Delta f = -16$ Hz). As Q_{mech} in balance at $\Delta f = -16$ Hz was estimated to be of order of a few hundred thousand, the magnitude of which is ignored in Fig. 4, the deviation of the red curve from the dashed line representing the linear change in $1/Q_{Joule}$ is most likely ascribed to the decrease in Q_{mech} from the imbalance of the two prongs. The plot at 0 Hz for the retuned fork sensor corresponded to $1/Q_{ele}$ of about 1/60 000; this value agreed with that estimated using plots around $f_{RT0} - f_{TF} = 0$ Hz in Fig. 3(b). The difference in $1/Q$ between the qPlus sensor and the retuned fork sensor can be ascribed to the dissipation in the oscillation energy at the join of the two prongs, estimated to be about 1/15 000, as indicated by $1/Q_{mech\_qPlus}$ in Fig. 4.

Concerning the improvement of the minimum detection limit $\delta F'_{min}$ according to Eq. (1), the Q factor of a two-prong type should noticeably be larger than twice that of a one-prong type, because the spring constant of the two-prong-type force sensor is practically twice as large as that of the one-prong-type force sensor.[17] While the Q factor for our qPlus sensor was about 10 000 in UHV, as large as typical values of 5000–15 000 reported in the literature, the Q factor of our retuned fork sensor even in a range of $f_{RT0} \pm 500$ Hz was larger than 30 000 in UHV. The Q_{mech} factor of the retuned fork sensor reached high enough for atom-resolved nc-AFM imaging, although there is room for improvement in terms of the detection circuit, which limited the Q_{eff} factor.

In summary, we demonstrated the performance of a retuned fork sensor for nc-AFM with atomic resolution, developed based on a quartz tuning fork with two prongs. To retune the resonance frequency of a one prong having an AFM tip to that of the other intact prong, we cut a small notch into one prong that improved immensely the Q factor of the sensor. We measured the Q factor decomposing it by dissipation channels to obtain estimates. The high Q factor of the retuned fork sensor is expected to enable dissipation signals between tip and sample to be acquired with high sensitivity.

This work was supported by Grants-in-Aid for Scientific Research (Nos. 24340068, 26630330, and 24246014) from the Japanese Society for the Promotion of Science.

[1]T. R. Albrecht, P. Grütter, D. Horne, and D. Rugar, J. Appl. Phys. **69**, 668 (1991).
[2]F. J. Giessibl, Science **267**, 68 (1995).
[3]T. Arai and M. Tomitori, Phys. Rev. Lett. **93**, 256101 (2004).
[4]F. J. Giessibl, Appl. Phys. Lett. **78**, 123 (2001).
[5]F. J. Giessibl, Phys. Rev. B **56**, 16010 (1997).
[6]W. H. J. Rensen, N. F. van Hulst, A. G. T. Ruiter, and P. E. West, Appl. Phys. Lett. **75**, 1640 (1999).
[7]F. J. Giessibl, Appl. Phys. Lett. **73**, 3956 (1998).
[8]F. J. Giessibl, Appl. Phys. Lett. **76**, 1470 (2000).
[9]A. Castellanos-Gomez, N. Agraït, and G. Rubio-Bollinger, Nanotechnology **21**, 145702 (2010).
[10]R. D. Grober, J. Acimovic, J. Schuck, D. Hessman, P. J. Kindlemann, J. Hespanha, A. S. Morse, K. Karrai, I. Tiemann, and S. Manus, Rev. Sci. Instrum. **71**, 2776 (2000).
[11]T. Arai and M. Tomitori, Jpn. J. Appl. Phys., Part 1 **39**, 3753 (2000).
[12]A. J. Weymouth, T. Wutscher, J. Welker, T. Hofmann, and F. J. Giessibl, Phys. Rev. Lett. **106**, 226801 (2011).
[13]J. Rychen, PhD dissertation, Swiss Federal Institute of Technology, Zurich, 2001.
[14]C. Zener, Phys. Rev. **52**, 230 (1937).
[15]S. Hudlet, M. S. Jean, C. Guthmann, and J. Berger, Eur. Phys. J. B **2**, 5 (1998).
[16]F. J. Giessibl, Rev. Mod. Phys. **75**, 949 (2003).
[17]F. J. Giessibl, F. Pielmeier, T. Eguchi, T. An, and Y. Hasegawa, Phys. Rev. B **84**, 125409 (2011).